



Internal variability in a coupled general circulation model in radiative-convective equilibrium

David Coppin, Sandrine Bony

► To cite this version:

David Coppin, Sandrine Bony. Internal variability in a coupled general circulation model in radiative-convective equilibrium. *Geophysical Research Letters*, 2017, 44 (10), pp.5142-5149. 10.1002/2017GL073658 . hal-02084813

HAL Id: hal-02084813

<https://hal.sorbonne-universite.fr/hal-02084813>

Submitted on 23 Oct 2021

HAL is a multi-disciplinary open access archive for the deposit and dissemination of scientific research documents, whether they are published or not. The documents may come from teaching and research institutions in France or abroad, or from public or private research centers.

L'archive ouverte pluridisciplinaire **HAL**, est destinée au dépôt et à la diffusion de documents scientifiques de niveau recherche, publiés ou non, émanant des établissements d'enseignement et de recherche français ou étrangers, des laboratoires publics ou privés.

Copyright

RESEARCH LETTER

10.1002/2017GL073658

Key Points:

- Internal variability arises in coupled radiative-convective equilibrium
- Ocean-atmosphere coupling affects phase relationships between temperature and aggregation
- Coupled RCE framework might help understand basic modes of tropical variability

Supporting Information:

- Supporting Information S1

Correspondence to:

D. Coppin,
d.coppin@auckland.ac.nz

Citation:

Coppin, D., and S. Bony (2017), Internal variability in a coupled general circulation model in radiative-convective equilibrium, *Geophys. Res. Lett.*, 44, 5142–5149, doi:10.1002/2017GL073658.

Received 29 MAR 2017

Accepted 11 MAY 2017

Accepted article online 16 MAY 2017

Published online 29 MAY 2017

©2017. The Authors.

This is an open access article under the terms of the Creative Commons Attribution-NonCommercial-NoDerivs License, which permits use and distribution in any medium, provided the original work is properly cited, the use is non-commercial and no modifications or adaptations are made.

Internal variability in a coupled general circulation model in radiative-convective equilibrium

David Coppin^{1,2} and Sandrine Bony¹
¹Laboratoire de Météorologie Dynamique, Sorbonne Université, UPMC Univ Paris 06, CNRS, Paris, France, ²Department of Physics, University of Auckland, Auckland, New Zealand

Abstract Numerical models run in non-rotating radiative-convective equilibrium (RCE) using prescribed sea surface temperatures (SSTs) show that convection can spontaneously aggregate into dry and moist areas, and that convective aggregation tends to increase with temperature. Using a general circulation model coupled to an ocean mixed layer, we show that in RCE the coupled ocean-atmosphere system exhibits some internal variability. This variability arises from the interplay between mean surface temperature, SST gradients and convective aggregation, and its timescale is proportional to the depth of the ocean mixed layer. For an ocean layer deeper than 10 m, the variability occurs at the interannual timescale, and variations of convective aggregation are almost out of phase with those of surface temperature. The coupled RCE framework might be relevant to understand some internal modes of variability of the tropical ocean-atmosphere system such as El Niño Southern Oscillation.

1. Introduction

The tendency of convection to aggregate has long been shown to influence the atmospheric circulation, especially through a modification of the vertical profiles of heating [Houze, 1982]. Subsequently, the study of convective aggregation with cloud-resolving models and observations shed light on its potential impact on climate. It was demonstrated that, when convection spontaneously self-aggregates in the absence of external drivers, it affects the mean large-scale atmospheric state: the atmosphere is drier and clearer [Bretherton et al., 2005; Tobin et al., 2012, 2013] and it radiates more heat to space [Khairoutdinov and Emanuel, 2010; Tobin et al., 2013]. Models forced by prescribed sea surface temperatures also suggest that aggregation increases as the surface warms [Khairoutdinov and Emanuel, 2010; Coppin and Bony, 2015; Bony et al., 2016], raising the question as to whether convective aggregation matters for climate change [Bony et al., 2015; Mauritsen and Stevens, 2015].

Most of the idealized studies investigating self-aggregation used the radiative-convective equilibrium (RCE) configuration with prescribed sea surface temperatures (SST). In this case, once convection is aggregated, it remains almost motionless. Indeed, Tompkins [2001] showed that with fixed SSTs, the displacement speed of convection is controlled by the rate of convective moistening of the free troposphere. When the atmosphere is coupled to an ocean mixed layer, on the other hand, convection moves around more rapidly [Grabowski, 2006; Reed et al., 2015]: convection is allowed to propagate rapidly toward the high SSTs in order to counteract the convection-SST feedback through which convection developing over warm regions suppresses solar insolation and increases surface turbulent fluxes, leading to a cooling of the local SST [Grabowski, 2006]. When coupled to a shallow mixed layer ocean, the triggering of self-aggregation can be either prevented [Hohenegger and Stevens, 2016] or delayed [Bretherton et al., 2005; Hohenegger and Stevens, 2016]. Once convection is aggregated, the coupling with an interactive SST leads to a breakup of the very large convective clusters found with fixed SSTs and increases the spatial variability of convection [Reed et al., 2015].

Therefore, multiple pieces of evidence suggest that ocean-atmosphere coupling affects the organization of convection. In this study, we investigate the impact that this coupling exerts on the global climate by examining the interaction between convective aggregation and surface temperature, and its relationship to the mean radiation budget of the Earth. We (i) describe the experimental setup and the different experiments, (ii) explore the relationship between mean surface temperature, SST gradients, and convective aggregation, and (iii) highlight a feedback loop that is associated with an internal mode of variability of the slab mean surface temperature.

2. Model and Methods

We run the LMDZ5A [Hourdin *et al.*, 2006] GCM, the atmospheric component of the IPSL-CM5A-LR coupled ocean-atmosphere model (for a detailed description of LMDZ5A-LR GCM, see Hourdin *et al.* [2006] and Dufresne *et al.* [2013], and references therein), in the same non-rotating RCE configuration as in Coppin and Bony [2015]. RCE is the statistical equilibrium state the atmosphere and surface would reach in the absence of lateral energy transport [Emanuel *et al.*, 2014]. This framework is widely used to understand the basic properties of the tropical atmosphere.

The model is used in an aquaplanet configuration without rotation and uses a latitudinal discretization in sine of latitude to ensure that the grid mesh area is uniform over the globe. It is forced by a constant and uniform insolation (1066.78 W/m^2 with a zenith angle corresponding to 0° latitude and a diurnal cycle). The ocean albedo is set to 0.07. The stratospheric ozone distribution is invariant and globally uniform (set to its mean equatorial profile). Aerosol effects are not considered.

The only difference between this study and Coppin and Bony [2015] comes from the use of an ocean mixed layer of 10 m depth instead of fixed and uniform SSTs. When the GCM is coupled to a slab ocean, the atmosphere and the ocean are thermodynamically coupled. Internal climate variability is driven solely by the thermal coupling between the ocean and the atmosphere, through radiative and turbulent fluxes at the surface. There is no ocean heat transport in this RCE framework. We considered different depths of the slab ocean ($H = 10, 20, 50$, and 100 m) and chose 10 m as it allowed us to simulate a global mean climate representative of deeper experiments (larger H) but reach the equilibrium faster. RCE experiments last 50 years except for the 50 m and 100 m slab experiments for which the experiments are run for 100 years. The first 10 years are usually discarded from the analysis, unless specifically mentioned. They are conceptually similar to those performed by Popke *et al.* [2013], Reed *et al.* [2015], and Hohenegger and Stevens [2016].

We also run a simulation in which the CO_2 concentration is abruptly doubled and then held constant.

3. Results

3.1. Interplay Between the Temperature and Convective Aggregation

When forced by an abrupt doubling of CO_2 concentration, the climate progressively warms and this long-term warming is associated with an increase in convective aggregation (blue and red lines in Figure 1b). The degree of aggregation is quantified using the subsidence fraction, SF, defined as the fraction of the domain with subsidence at 500 hPa [Coppin and Bony, 2015]. The blue line corresponds to SF smoothed over 75 days using a convolution method. This simultaneous increase and maintenance in both aggregation and global mean temperature is consistent with prescribed SST experiments [Coppin and Bony, 2015; Bony *et al.*, 2016].

What is more surprising is the fact that, both in control and $2\times\text{CO}_2$ experiments, surface temperature exhibits short-term variations of SF, out of phase with rapid variations of global mean surface temperature. These variations are associated with significant variations (up to 8 W/m^2) of the globally averaged radiative budget at the top of the atmosphere (Figures 1c and 1d). A maximum in aggregation (or SF) is generally associated with a minimum in global mean surface temperature.

Therefore, the relationship between convective aggregation and surface temperature appears to be different on long and short timescales. Hereafter, we investigate the factors controlling it on short timescales.

To understand the interplay between convective aggregation and SST, we examine the precipitation pattern, closely related to convection, as a function of time and surface temperature (Figures 2a and 2b). In these figures, the maximum of aggregation over 24 consecutive months (with a moving window of 12 months) is indicated by a filled blue dot on the right of the figure (same dots as in Figures 1a and 1b). We clearly notice a propagation of convection from regions of intermediate SST to warm regions, with a peak of aggregation occurring when convection is over the highest SST. Just after the maximum of aggregation, convection disappears from the warm regions and pops up in regions of intermediate SST before moving toward the warm SSTs again.

To find out what controls this cycle, we build composites of $\overline{T_s}$, SF, σ_{T_s} , the standard deviation of T_s (a proxy for SST gradients), clear-sky (CS) outgoing longwave radiation (OLR), the fraction of low clouds in subsiding regions (f_L), and the latent heat flux (LHF) over a 24 month period centered around the maximum of

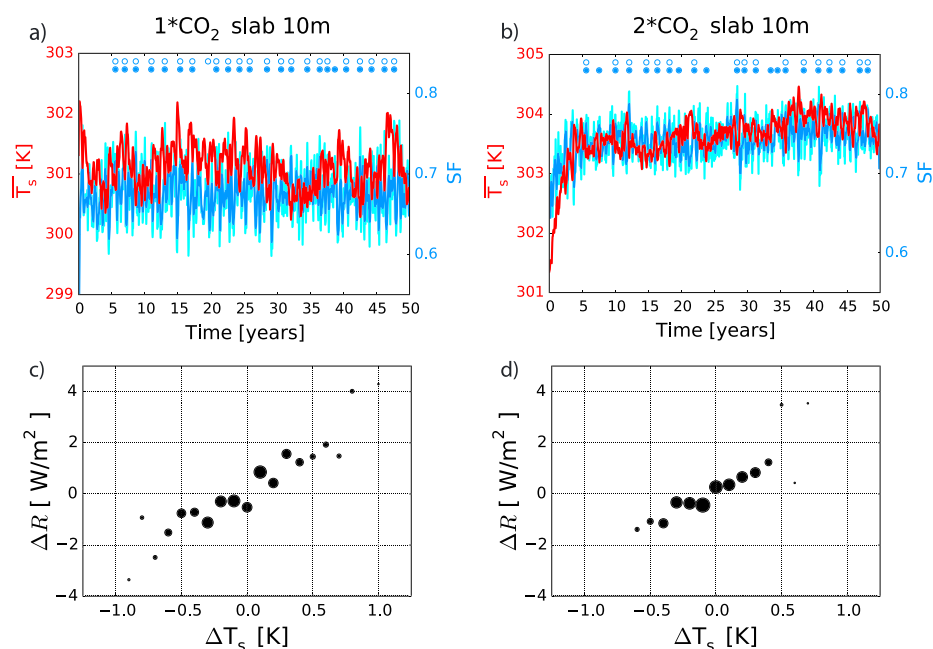


Figure 1. Top line: time evolution of global mean surface temperature (red) and subsidence fraction (SF, monthly averaged in light blue and smoothed over one third of the oscillation in darker blue) for the 10m-slab experiment with (a) preindustrial CO₂ concentration and (b) abruptly doubled CO₂ concentration. Bottom line: top of atmosphere (TOA) net radiative budget binned by 0.1 K SST anomalies relative to the global mean equilibrium temperature for the same experiment with (c) preindustrial CO₂ concentration and (d) abruptly doubled CO₂ concentration. Radiative and temperature anomalies are calculated relative to the global mean over the last 40 years of each simulation. Data are monthly averaged. In Figures 1a and 1b, full blue dots show local maxima of aggregation for each consecutive ensemble over 24 months. Open blue dots show local maxima of SF stronger than one standard deviation. See Methods S1 in the supporting information for further details.

SF (Figures 2c and 2d). The conclusions drawn from these figures and our visual inspection of the simulation are summarized in Figure 3. They remain similar when composited only from aggregation maxima (see Methods S1).

The most distinct feature is that, around equilibrium, convective aggregation is nearly out of phase with global mean surface temperature (Figure 3c). Three to six months prior to the maximum of aggregation (lag = 0 month in Figures 2c and 2d), a period of maximum SST is associated with a minimum aggregation (Figure 3a). At the end of this warm period, convection starts moving toward the areas that were previously clear and whose surface has been warmed by solar radiation because the stronger surface warming over the clear-sky areas created an SST gradient that drives a large-scale circulation. The strong wind at the surface increases the latent heat fluxes behind the moving convection zones, cooling the surface, and increasing even more the gradient between the warm unperturbed regions and the cold regions (Figure 3b). The strong circulation keeps amplifying with increasing aggregation, causing a drying of the free troposphere (maximum OLR). In parallel, the strong subsidence favors the formation of low clouds over cold SSTs. Convection keeps moving until it concentrates in one area of the domain (Figure 3c). This time corresponds to the maximum of low clouds generated by the strong subsidence and the minimum of surface temperature (due to the combined effect of increased OLR, SW reflection by low clouds over the cold regions, and decaying LHF close to the previously warm regions). Once convection occurs over the warmest spot, it cannot move somewhere else. Since the SST has been homogenized by the displacement of convection while aggregating, SST gradients are weak. Convection ends up dying, which kills the large-scale circulation and eventually the low clouds. Without circulation and after a delayed period during which the surface temperature remains low, clear-sky areas warm due to the incoming SW radiation and convection develops in multiple parts of the domain where SST gradients start to emerge. Convection does not sustain itself long over the warmest SSTs (Figures 2a and 2b) because its shading effect lowers the underlying SST quickly (convection then becomes associated with intermediate SSTs). Finally, the system warms up until it comes back to its starting point (Figure 3a). The feedback loop lasts between 7 and 8 months for $H = 10$ m.

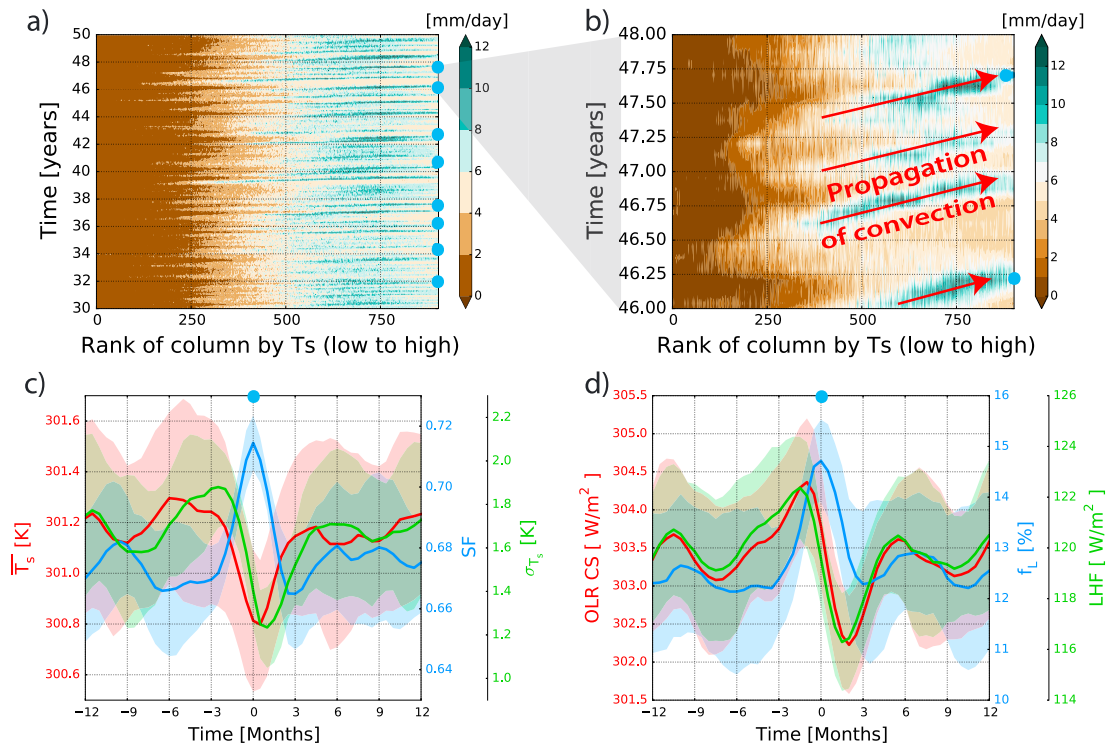


Figure 2. (a) Precipitation between year 30 and 50 of the simulation with 1CO_2 and a 10 m slab depth as a function of surface temperature and time. The different grid points of the model are classified according to their surface temperature (coldest on the left, warmest on the right). Ten consecutive points are averaged to give a single precipitation value. Maximum aggregation is indicated by blue dots (maximum of 24 consecutive months). (b) Zoom between year 46 and 48 of the same simulation showing the propagation of convective clouds toward warm SSTs. (c) Composites of the global mean surface temperature \bar{T}_s (red), SF (blue), and the standard deviation of the SST σ_{T_s} (green) over 24 months for the last 40 years of simulation. Composites are centered around the maximum of SF (blue dots in Figures 2a and 2b). A negative time refers to events occurring before the maximum of SF. Shading indicates the standard deviation at each time. (d) Same as Figure 2c for the clear-sky OLR (red), the fraction of low clouds in subsiding regions (blue) and the latent heat flux (green).

When the CO_2 concentration is doubled, although the climate is 2.5 K warmer and the aggregation stronger (Figure S2), the feedback loop between convective aggregation and global mean surface temperature remains the same. Thus, the general structure of the feedback loop does not seem to depend strongly on the mean climate state. However, analyzing the 2CO_2 - 1CO_2 composites gives a few hints on how it can be partially modified in a warmer climate (Figure S3 and discussion in Methods S3). The amplitude of the aggregation change is stronger with 1CO_2 concentration and a higher low-cloud fraction, possibly indicating that the positive feedback of low clouds associated with a CO_2 doubling in our model [Brient and Bony, 2012; Vial et al., 2013, 2016] can damp the feedback loop, reduce the increase in convective aggregation, and limit its cooling effect in a warming climate.

3.2. Dependence on Ocean Mixed Layer Depth

Changing the depth of the ocean mixed layer H affects the timescale of the oscillation period (Figure S4) but does not change the general sequence of events (Figures 4 and S5; see Methods S2 for details). As H increases, the thermal inertia of the ocean increases and the feedback loop occurs over a longer timescale: from 7 to 8 months for a 10 m slab to 6 to 7 years for the 100 m slab. The length of the cycle is directly proportional to H . The delay between the minimum of global mean surface temperature and the maximum of aggregation appears more clearly as H increases (Figure 4). Since aggregation and global surface temperature are less and less out of phase when the slab depth increases, the slopes between monthly averaged ΔR and ΔT_s gradually weaken (Figure S6).

To understand the robust relationships between convective aggregation and global mean surface temperature, as well as the proportional increase in the oscillation period, we express the time evolution of the surface temperature of the coupled system as

$$\rho_w c_w H \frac{d\bar{T}_s}{dt} = -\bar{F}_s - \bar{F}_L + \bar{R}_{SW} + \bar{R}_{LW} = \bar{Q} \quad (1)$$

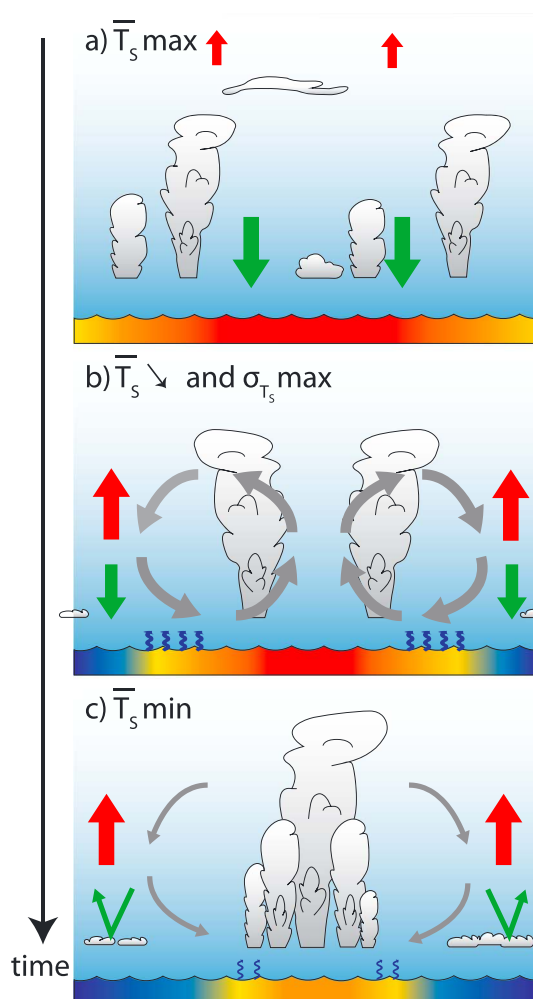


Figure 3. (a) Schematic of the mean state when the mean surface temperature is maximum and SF minimum. (b) Schematic when the SST gradients are maximum and convection organizing while moving toward the warm SSTs. (c) Schematic when self-aggregation is maximum and the mean surface temperature approaches its minimum owing to LW_{CS} heat loss and partial reflection of SW radiation by low clouds.

with $\rho_w = 10^3 \text{ kg m}^{-3}$ the water density, $c_w = 4.3 \text{ J kg}^{-1} \text{ K}^{-1}$ the specific heat of water, F_s and F_L the sensible and latent heat fluxes at the surface, R_{SW} and R_{LW} the net shortwave and longwave fluxes at the surface, and H the slab depth. Overlines represent global averages. In the following, overlines are removed but we always consider global averages.

At first approximation, T_s and Q oscillate at the same frequency but T_s exhibits a phase shift relative to Q (Figure 4). Thus, we assume that both T_s and Q are sinusoidal functions with frequency ω and a phase shift ϕ between them: $Q = Q_0 e^{i\omega t}$ and $T = T_0 e^{i(\omega t + \phi)}$. Q_0 and T_0 represent the maximum amplitude of Q and global surface temperature, respectively. This formulation furthermore assumes that the phase relationship between aggregation and temperature is independent of the reference climate state. Since radiative and surface fluxes are strongly influenced by convective aggregation, especially for deeper H where Q and SF are anticorrelated (Figure 4), Q directly relates to convective aggregation.

Replacing equation (1) with the sinusoidal equations and separating real and imaginary parts gives the following system of equations:

$$\begin{cases} \rho_w c_w H \omega T_0 \sin(\phi) = -Q_0 \\ \rho_w c_w H \omega T_0 \cos(\phi) = 0 \end{cases} \quad (2)$$

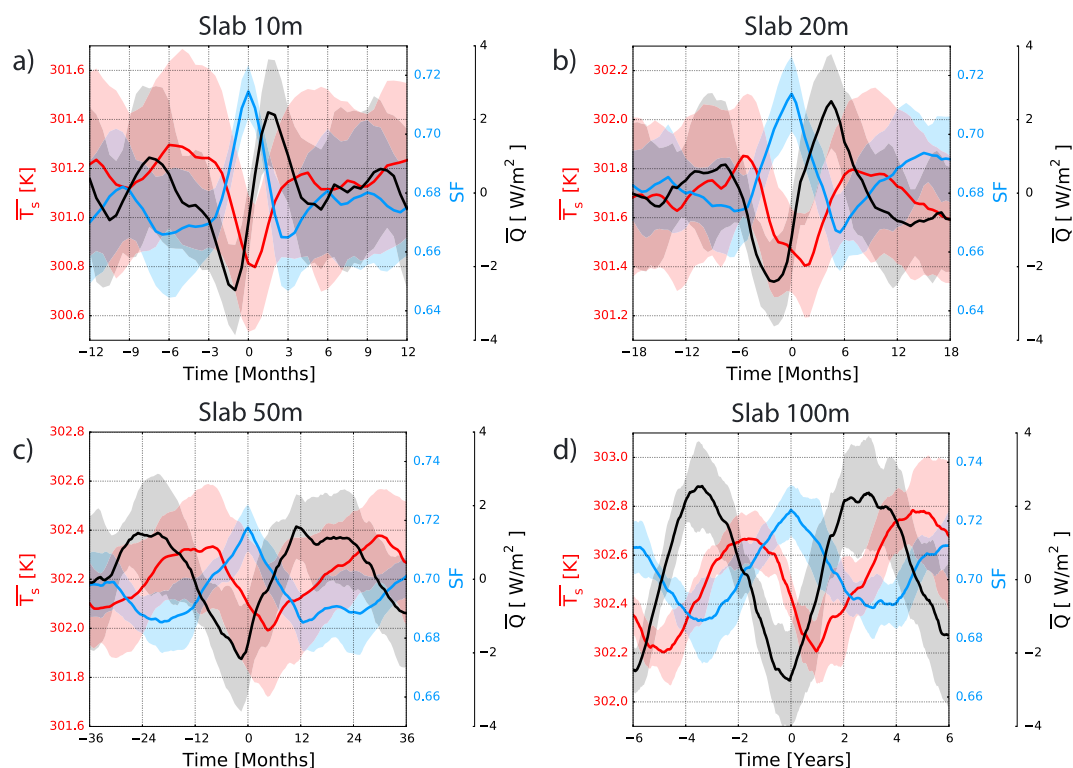


Figure 4. Similar to Figure 2c with \bar{Q} (black line) instead of SST gradients, for a depth of the ocean mixed layer of (a) 10 m, (b) 20 m, (c) 50 m, and (d) 100 m, and a preindustrial CO_2 concentration.

Solving (2) leads to

$$\phi = -\frac{\pi}{2} \quad (3)$$

and

$$\omega = \frac{Q_0}{\rho_w c_w H T_0} \quad (4)$$

Hence, the term Q (and aggregation that relates to it) is expected to be in phase quadrature with Q leading the global surface temperature. This is verified by Figure 4 for the deep (50 m and 100 m) ocean mixed layer depths. For the smaller ones, Q is also in phase quadrature with the global surface temperature. But, due to the phase shift between Q and SF , this is not really the case between aggregation and surface temperature.

Consistent with the values observed in those figures, equation (4) gives an oscillation period of 7.9, 14.4, 40.3, and 72.0 months for $H = 10, 20, 50$, and 100 m, respectively. Equation (4) also explains why a proportionality exists between the oscillation periods depending on the slab depth. As $\frac{Q_0}{T_0}$ turns out to be nearly invariant as H varies, ω is directly proportional to H .

4. Conclusions and Discussion

This study shows that a coupled ocean-atmosphere system in radiative-convective equilibrium exhibits some internal variability which results from the ocean-atmosphere coupling. This coupling arises from the interplay between convective aggregation, SST gradients and mean surface temperature, and its influence on turbulent and radiative heat fluxes at the ocean surface. This interplay shares similarities with the convection-SST feedback discussed by Grabowski [2006]. It is robust to a doubling of the CO_2 concentration and to a change of the ocean mixed layer depth by a factor of 10.

This study also shows that in a coupled framework, the relationship between convective aggregation and global-mean surface temperature depends on the timescale under consideration: while aggregation tends

to vary in phase with surface temperature on long (multidecadal) timescales, it can be nearly out of phase on shorter (interannual) timescales. For these short timescales, the period of the feedback loop is directly proportional to the depth of the ocean mixed layer depth.

Both the phenomenology and the timescale of the deep slab experiments resemble results from less idealized AGCM-slab experiments [Dommenget, 2010; Dommenget et al., 2014], in which atmospheric GCMs (with continents, rotation, and a meridional distribution of insolation) are coupled to a slab ocean and forced by twentieth century boundary conditions. Even though the timescales are longer, the dynamics leading the transition from slab El Niño to decaying El Niño or La Niña present a sequence of events that is similar to those controlling our feedback loop with aggregation. Interestingly, changing the slab depth from 50 m to 20 m or 100 m also proportionally alter the timescale of the variability.

The RCE framework has long been recognized as a powerful tool to explain the thermal structure of the tropical atmosphere. This study raises the question whether coupled RCE might be a relevant framework to understand some basic modes of internal variability of the tropical climate. The resemblance between the results of this study and previous investigations of the mechanisms of internal variability of the coupled system in less idealized frameworks [Dommenget, 2010; Clement et al., 2011; Bellomo et al., 2014, 2015; Clement et al., 2015] suggests that the fundamental coupling between the organization of convection and SSTs highlighted in this study may contribute to the interannual variability of the tropical atmosphere and lead to the development of ENSO events.

Acronyms

RCE	Radiative-Convective Equilibrium
SST	Sea Surface Temperature
CRM	Cloud-Resolving Model
GCM	General Circulation Model
SF	Subsiding Fraction
CS	Clear Sky
LW	Longwave
OLR	Outgoing Longwave Radiation
f_L	Fraction of low clouds in subsiding regions
LHF	Latent Heat Flux

Acknowledgments

We thank Adrian Tompkins, Cathy Hohenegger, Caroline Muller, Jean-Pierre Chaboureaud, and Jean-Yves Grandpeix for many useful discussions during the development of this work. We also want to thank the two reviewers for their constructive comments. This work was granted access to the HPC resources of the Institut du développement et des ressources en informatique scientifique (IDRIS) under the allocation 0292 made by GENCI. We acknowledge support from UPMC (Université Pierre et Marie Curie) and the European Research Council (ERC) EUREC⁴A grant 694768. All the data used in this study are available at: ftp://ftp.lmd.jussieu.fr/pub/dcoppin/data_article_var_rce/.

References

- Bellomo, K., A. Clement, T. Mauritsen, G. Radel, and B. Stevens (2014), Simulating the role of subtropical stratocumulus clouds in driving Pacific climate variability, *J. Clim.*, 27, 5119–5131, doi:10.1175/JCLI-D-13-00548.1.
- Bellomo, K., A. Clement, T. Mauritsen, G. Radel, and B. Stevens (2015), The influence of cloud feedbacks on equatorial Atlantic variability, *J. Clim.*, 28, 2725–2744, doi:10.1175/JCLI-D-14-00495.1.
- Bony, S., et al. (2015), Clouds, circulation and climate sensitivity, *Nat. Geosci.*, 8(4), 261–268, doi:10.1038/ngeo2398.
- Bony, S., B. Stevens, D. Coppin, T. Becker, K. A. Reed, A. Voigt, and B. Medeiros (2016), Thermodynamic control of anvil cloud amount, *Proc. Natl. Acad. Sci.*, 113(32), 8927–8932.
- Bretherton, C. S., P. N. Blossey, and M. Khairoutdinov (2005), An energy-balance analysis of deep convective self-aggregation above uniform SST, *J. Atmos. Sci.*, 62(12), 4273–4292, doi:10.1175/JAS3614.1.
- Brient, F., and S. Bony (2012), How may low-cloud radiative properties simulated in the current climate influence low-cloud feedbacks under global warming?, *Geophys. Res. Lett.*, 39, L20807, doi:10.1029/2012GL053265.
- Clement, A., P. Di Nezio, and C. Deser (2011), Rethinking the ocean's role in the Southern Oscillation, *J. Clim.*, 24(1969), 4056–4072, doi:10.1175/2011JCLI3973.1.
- Clement, A., K. Bellomo, L. N. Murphy, M. A. Cane, T. Mauritsen, and B. Stevens (2015), The Atlantic Multidecadal Oscillation without a role for ocean circulation, *Science*, 350(6258), 320–324.
- Coppin, D., and S. Bony (2015), Physical mechanisms controlling the initiation of convective self-aggregation in a general circulation model, *J. Adv. Model. Earth Syst.*, 7, 2020–2078, doi:10.1002/2013MS000282.Received.
- Dommenget, D. (2010), The slab ocean El Niño, *Geophys. Res. Lett.*, 37, L20701, doi:10.1029/2010GL044888.
- Dommenget, D., S. Haase, T. Bayr, and C. Frauen (2014), Analysis of the slab ocean El Niño atmospheric feedbacks in observed and simulated ENSO dynamics, *Clim. Dyn.*, 42, 3187–3205, doi:10.1007/s00382-014-2057-0.
- Dufresne, J. L., et al. (2013), Climate change projections using the IPSL-CM5 Earth System Model: From CMIP3 to CMIP5, *Clim. Dyn.*, 40, 2123–2165, doi:10.1007/s00382-012-1636-1.
- Emanuel, K. A., A. A. Wing, and E. M. Vincent (2014), Radiative-convective instability, *J. Adv. Model. Earth Syst.*, 6(1), 75–90, doi:10.1002/2013MS000270.
- Grabowski, W. W. (2006), Impact of explicit atmosphere-ocean coupling on MJO-like coherent structures in idealized aquaplanet simulations, *J. Atmos. Sci.*, 63, 2289–2306.
- Hohenegger, C., and B. Stevens (2016), Coupled radiative convective equilibrium simulations with explicit and parameterized convection, *J. Adv. Model. Earth Syst.*, 8(3), 1468–1482, doi:10.1002/2013MS000282.Received.

- Hourdin, F., et al. (2006), The LMDZ4 general circulation model: Climate performance and sensitivity to parametrized physics with emphasis on tropical convection, *Clim. Dyn.*, 27(7-8), 787–813, doi:10.1007/s00382-006-0158-0.
- Houze, R. A. (1982), Cloud clusters and large-scale vertical motions in the tropics, *J. Meteorol. Soc. Jpn. II*, 60(1), 396–410.
- Khairoutdinov, M., and K. A. Emanuel (2010), Aggregated convection and the regulation of tropical climate, paper P2.69 presented at the 29th Conference on Hurricanes and Tropical Meteorology, Tucson, Ariz., May. [Available online at http://ams.confex.com/ams/29Hurricanes/techprogram/paper_168418.htm.]
- Mauritsen, T., and B. Stevens (2015), Missing iris effect as a possible cause of muted hydrological change and high climate sensitivity in models, *Nat. Geosci.*, 8(April), 8–13, doi:10.1038/ngeo2414.
- Popke, D., B. Stevens, and A. Voigt (2013), Climate and climate change in a radiative-convective equilibrium version of ECHAM6, *J. Adv. Model. Earth Syst.*, 5(1), 1–14, doi:10.1029/2012MS000191.
- Reed, K. A., B. Medeiros, J. T. Bacmeister, and P. H. Lauritzen (2015), Global radiative-convective equilibrium in the community atmosphere model, version 5, *J. Atmos. Sci.*, 72(5), 2183–2197, doi:10.1175/JAS-D-14-0268.1.
- Tobin, I., S. Bony, and R. Roca (2012), Observational evidence for relationships between the degree of aggregation of deep convection, water vapor, surface fluxes, and radiation, *J. Clim.*, 25(20), 6885–6904, doi:10.1175/JCLI-D-11-00258.1.
- Tobin, I., S. Bony, C. E. Holloway, J.-Y. Grandpeix, G. Sèze, D. Coppin, S. J. Woolnough, and R. Emy Roca (2013), Does convective aggregation need to be represented in cumulus parameterizations?, *J. Adv. Model. Earth Syst.*, 5, 692–703, doi:10.1002/jame.20047.
- Tompkins, A. (2001), On the relationship between tropical convection and sea surface temperature, *J. Clim.*, 14, 633–637, doi:10.1175/1520-0442(2001)014<0633:OTRBTC>2.0.CO;2.
- Vial, J., J. L. Dufresne, and S. Bony (2013), On the interpretation of inter-model spread in CMIP5 climate sensitivity estimates, *Clim. Dyn.*, 41(11-12), 3339–3362, doi:10.1007/s00382-013-1725-9.
- Vial, J., S. Bony, J.-L. Dufresne, and R. Roehrig (2016), Coupling between lower-tropospheric convective mixing and low-level clouds: Physical mechanisms and dependence on convection scheme, *J. Adv. Model. Earth Syst.*, 8, 1892–1911, doi:10.1002/2016MS000740.